

# Using Multivariate Singular Spectrum Analysis for Estimating Trends in Global Climate Change Indicators

Mahdi Haddad

Department of Space Geodesy - Centre of Space Techniques  
1 Avenue de la Palestine. BP 13 Arzew. Oran 31200, Algeria  
e-mail: mhaddad@cts.asal.dz

**Abstract**—This paper aims to explore temporal variability of three major changes scientists have seen in our climate system: Global Mean Sea Level (GMSL), global land-ocean temperature and atmospheric carbon dioxide concentrations. These three time series (variables) are used to investigate observed trends with Multivariate Singular Spectrum analysis (MSSA) model. Evidence of this study demonstrates that global mean sea level has been rising during the satellite altimetry era (1993-2015) by 3.36 mm/year. Average global land-ocean temperatures increased 0.39°C, while the average rate of increase in the atmospheric CO<sub>2</sub> content recorded at Mauna Loa is 1.98 ppm/year over the considered period (1993-2015).

**Keywords**-Multivariate Singular Spectrum Analysis; Global climate change; Time series decomposition; Global mean sea level; Global land-ocean temperature; Atmospheric carbon dioxide.

## I. INTRODUCTION

When we speak about "global warming", which has become progressively and insidiously "climate change", it is generally a question of global phenomena that apply either to the whole earth or to large ensembles: hemispheres, lands, oceans, poles, etc. The first sign of global warming is obviously the global rise in temperature (of the atmosphere as well as of the oceans). This change leads to particularly serious consequences: climate disruptions (increased droughts and the collapse of agriculture in certain regions of the world, torrential rains, etc.), rising sea-water level, warming of the oceans, melting glaciers, accentuation of El Nino phenomenon, modification of the geographical distribution of fauna and flora, etc. The discovery of the climate change problem dates back to 1824 when the French physicist *Joseph Fourier* proposed a theory under which the temperature on Earth is accumulated by the atmosphere that traps a part of the infrared radiation emitted by the Earth [1]. This is a first draft of the greenhouse effect.

In order to understand and explain the glaciations cycle, Swedish chemist *Svante Arrhenius* drew up a theory in 1896 that links the increase in atmospheric carbon dioxide (CO<sub>2</sub>) to a significant increase in terrestrial temperatures by reason to the greenhouse effect due to water vapor and carbonic acid (dissolved CO<sub>2</sub> in water vapor) [2]. He indicated already with great foresight that the doubling of the carbon dioxide concentration in the atmosphere leads to an increase in temperature of 4° to 6°C, which corresponds roughly to current estimates.

In 1958, *Charles David Keeling* began to measure CO<sub>2</sub> concentrations on the *Mauna Loa* volcano in *Hawaii*; they then are 315 ppm [3]. In 1961, Keeling provided the measurement results, which gave rise to the famous Keeling curve, showing that CO<sub>2</sub> levels were rising sharply, a trend that has steadily increased since then. In 1979, the American National Academy of Sciences launched the first rigorous study on global warming. On the basis of this investigation, the *Charney's committee* responsible for it concluded that anthropogenic CO<sub>2</sub> emissions from industrial sources is the only cause of the catastrophic imbalance of the greenhouse effect and that the annual mean temperature will increase continuously as a result of the increase in CO<sub>2</sub> concentration [4].

Since 1988, several internationally-renowned researchers have met under United Nations auspices to form the Intergovernmental Panel on Climate Change – IPCC to work on climate change. Five reports have already been published in 1990, 1995, 2001, 2007 and 2014 [5]. All those reports affirm that the warming of the climate system is unequivocal, and that many of observed changes are unprecedented for decades, centuries or even millennia: warming of the atmosphere and oceans, reduced snow cover and widespread ice melting, sea-level rise, increasing concentrations of greenhouse gases, etc. In June 2004, a European team (European Project for Ice Coring in Antarctica) traced the history of our atmosphere over 740,000 years from investigations of ice cores from Antarctica. The analysis of air bubbles trapped in the ice confirms that current levels of greenhouse gases reached the highest level ever observed in the last 440,000 years [6].

Signed in 1997, the *Kyoto Protocol*, that is an international agreement, established according to the UN Framework Convention on Climate Change, meets the challenge of real and substantial reductions in greenhouse gas emissions [7]. With its entry into force in 2005, it had been ratified by 183 countries. The European Union, as well as countries likely to be directly affected by the threat and potential consequences of climate change, have been the most ardent defenders of the plan. However, there is currently a controversy in the international scientific community on climate change. The stone into the pond was launched when more than 31,000 US scientists signed a text claiming that there is no tangible evidence that CO<sub>2</sub> emissions are likely to cause a catastrophic rise in temperatures on Earth [8].

This study aims to investigate the main behavior of the ocean surface variability in relation to the two key indicators of climatic warming, namely the global land-ocean mean temperature and carbon dioxide (CO<sub>2</sub>) concentrations in the atmosphere, by use of the Multivariate Singular Spectrum Analysis (MSSA) technique that is a straightforward extension of the basic Singular Spectrum Analysis (SSA). For this purpose, a multivariate system composed by three time series (1993-2015) has been investigated: GMSL, Global land-ocean mean temperature anomalies and CO<sub>2</sub> concentrations measured at *Mauna Loa*. The result of the MSSA processing is a decomposition of these time series into several components, which can be identified as trend, seasonalities and noise components.

The paper is structured as follows. Section 2 provides a description on MSSA as a multidimensional version of SSA; the used datasets are described in Section 3. Section 4 offers analysis and empirical findings of the paper by using MSSA modeling with concluding remarks on the findings in Section 5.

## II. METHODOLOGY - REMINDERS ABOUT MULTIVARIATE SINGULAR SPECTRUM ANALYSIS (MSSA)

In this section, we introduce the algorithm of MSSA as a multidimensional version of SSA, for analysis and forecasting of multivariate time series following the approach described in [9] for one-dimensional series and in [10] for multidimensional ones.

SSA is a nonparametric technique that works with arbitrary statistical processes, whether linear or nonlinear, stationary or non-stationary, Gaussian or non-Gaussian. The main idea of SSA is performing a Singular Value Decomposition (SVD) of the trajectory matrix obtained from the original time series with a subsequent reconstruction of the series. The basic version of SSA consists of five steps, which are performed as follows:

**Step 1. Embedding.** The first step consists in the construction of the so-called trajectory matrix ( $\mathcal{T}_{SSA}$ ) by associating a time series  $\mathbf{x} = (x_1, \dots, x_N)$  to  $(K = N - L + 1)$  column-vectors of dimension  $L$ , where  $L$  is the window length:

$$\mathcal{T}_{SSA} = \mathbf{X} = \begin{bmatrix} x_1 & x_2 & x_3 & \dots & x_k \\ x_2 & x_3 & x_4 & \dots & x_{k+1} \\ x_3 & x_4 & x_5 & \dots & x_{k+2} \\ \vdots & \vdots & \vdots & \ddots & \vdots \\ x_L & x_{L+1} & x_{L+2} & \dots & x_N \end{bmatrix} \quad (1)$$

Note that the trajectory matrix  $\mathbf{X}$  is a Hankel matrix, which means that all the elements along the diagonal  $i + j = \text{const}$  are equal.

**Step 2. Singular Value Decomposition.** Compute the eigenvalues and eigenvectors of the matrix  $S = \mathbf{X}\mathbf{X}^T$ . Let  $\lambda_1 \geq \dots \geq \lambda_L \geq 0$  be eigenvalues of the matrix  $S$ ,  $d = \max\{j: \lambda_j > 0\}$ ,  $(U_1, V_1); \dots; (U_d, V_d)$  the associated singular vectors left and right. The trajectory matrix  $\mathbf{X}$  can be written as [9]:

$$\mathbf{X} = \sum_{j=1}^d \mathbf{X}_j, \quad \text{with } \mathbf{X}_j = \sqrt{\lambda_j} U_j V_j^T \quad (2)$$

The triple  $(\sqrt{\lambda_j}, U_j, V_j)$  is called the  $j^{\text{th}}$  eigentriple.

**Step 3. Grouping.** This step partitions the  $X_j$  set of indices  $\{1, \dots, d\}$  into  $m$  disjoint subsets  $I_1, \dots, I_m$ . For a subset  $\{i_1, \dots, i_p\}$ , the matrix  $X_{I_1}$  corresponding to the group  $I$  is defined as:

$$X_I = X_{I_1} + \dots + X_{I_m} \quad (3)$$

**Step 4. Reconstruction of the one-dimensional series.** At this final step, each matrix of the decomposition “(3)” is transferred back to the form of the input object  $\mathbf{x}$ . Let the *Hankelization* operator  $\Pi^{(H)}$  be averaging of the corresponding diagonals of the matrix  $\hat{X}_k = X_{I_k}$  for  $i = 1, \dots, m$ . Thus, denote  $\tilde{X}_k = X_{I_k}$  the reconstructed matrices,  $\tilde{X}_k = \Pi^{(H)} \hat{X}_k$  the trajectory matrices of the reconstructed data and  $\tilde{\mathbf{x}}_k = \mathcal{T}^{-1} \tilde{X}_k$  the reconstructed data themselves. Then, the resultant decomposition of the initial data has the form:

$$\mathbf{x} = \tilde{\mathbf{x}}_1 + \dots + \tilde{\mathbf{x}}_m \quad (4)$$

Consider now a multivariate time series, that is, a collection  $\{\mathbf{x}^{(p)} = (x_j^{(p)})_{j=1}^{N_p}, p = 1, \dots, s\}$  of  $s$  time series of length  $N_p, p = 1, \dots, s$ . Denote  $\mathbf{x} = (\mathbf{x}^{(1)}, \dots, \mathbf{x}^{(s)})$  the initial data for the MSSA algorithm. Since the general scheme of the algorithm described for SSA holds for MSSA, we need to define the embedding operator  $\mathcal{T}_{MSSA}(\mathbf{x}) = \mathbf{X}$  only. Let  $L$  be the window length,  $1 < L < \min(N_p, p = 1, \dots, s)$ . For each time series  $\mathbf{x}^{(p)}$ , the embedding procedure forms  $K_p = N_p - L + 1$   $L$ -lagged vectors  $X_j^{(p)} = (x_j^{(p)}, \dots, x_{j+L-1}^{(p)})^T, 1 \leq j \leq K_p$ . Denote  $K = \sum_{p=1}^s K_p$ . The trajectory matrix of the multidimensional series is the  $L \times K$  matrix of the form [10]:

$$\mathcal{T}_{MSSA}(\mathbf{x}) = \mathbf{X} = \begin{bmatrix} X_1^{(1)} & \dots & X_{K_1}^{(1)} & \dots & X_1^{(s)} & \dots & X_{K_s}^{(s)} \\ \vdots & \dots & \vdots & \dots & \vdots & \dots & \vdots \end{bmatrix} = [\mathbf{X}^{(1)}; \dots; \mathbf{X}^{(s)}] \quad (5)$$

where  $\mathbf{X}^{(p)} = \mathcal{T}_{MSSA}(\mathbf{x}^{(p)})$  is the trajectory matrix of the one-dimensional series  $\mathbf{x}^{(p)}$  defined in “(2)”. Thus, the trajectory matrix of a system of time series has stacked Hankel structure. The eigenvectors  $\{U_i\}$  in the SVD (3) of  $\mathbf{X}$  form the common basis of the column trajectory spaces of all time series from the system. Factor vectors  $V_i$  (named EOF in climatology applications) consist of parts related to each time series separately, that is,

$$V_i = \begin{pmatrix} V_i^{(1)} \\ \vdots \\ V_i^{(s)} \end{pmatrix} \quad (6)$$

where  $V_i^{(p)} \in R^{K_p}$  and belong to the row trajectory spaces of the  $p^{\text{th}}$  series. The eigenvectors  $U_i$  reflect the common features of time series, while the factor subvectors  $V_i^{(1)}$  show how these common features appear in each series. It is natural to transform a factor vector to a factor system of factor subvectors  $V_i^{(p)}$ . Then, the form of transformed factor vectors will be similar to the initial system of series.

Analogously to the one-dimensional case, the main result of the application of MSSA is the decomposition “(4)” of the multivariate time series into a sum of  $m$  multivariate series.

### III. DATA

In this study, we consider a multivariate system composed by the three time series:

#### A. Global Mean Sea Level Reference

Radar altimeters permanently transmit signals to the Earth, and receive the reflected echo from the sea surface. The satellite orbit has to be accurately tracked and its position is determined relative to a reference surface (an ellipsoid). The sea surface height (SSH) is calculated by subtracting the measured distance between the satellite and sea surface from the precise orbit of the satellite. The sea level anomalies (SLA) are defined as variations of the sea surface height (SSH) with respect to an a priori mean sea surface (MSS). In this study, a temporal series of averaged sea level anomalies (SLA) over all oceans and seas for the entire altimetry period is used (1993-2015) (Fig. 1). This series is obtained by combining the time series from all three TOPEX, Jason-1 and Jason-2 missions and is provided by the CU Sea Level Research Group of the University of Colorado [11].

#### B. Global Land-Ocean Mean Temperature Anomalies

The three most highly cited combined land temperature and sea surface temperature (SST) data sets are NOAA's Merged Land-Ocean Surface Temperature (MLOST), NASA's GISTEMP, and the UK's HadCRUT. In this study, a temporal series of global land-ocean mean temperature anomalies from NOAA is used (Fig. 2). The MLOST datasets are spatially gridded ( $5^\circ \times 5^\circ$ ), with monthly resolution from January 1880 to present. The SST dataset is the Extended Reconstructed Sea Surface Temperature (ERSST) v 3b. The land surface air temperature dataset is similar to ERSST, but uses data from the Global Historical Climatology Network Monthly (GHCNM) database [12][13].

#### C. CO<sub>2</sub> Concentrations Measured at Mauna Loa

Monthly series of CO<sub>2</sub> concentrations in the atmosphere measured at the *Mauna Loa* Observatory in Hawaii (lat:  $19^\circ 32'10''$  N; Long:  $155^\circ 34'34''$  W), expressed in mole fraction in dry air (Fig. 3). All of the measurements are rigorously and very frequently calibrated (accuracy better than 0.2 ppm). Dated from 1958, *Mauna Loa* is the measuring station of the oldest atmospheric CO<sub>2</sub> in the world. We choose to use the CO<sub>2</sub> measurements made at the *Mauna Loa* Observatory because the Observatory near the summit of *Mauna Loa*, at an altitude of 3400 m, is well situated to measure air masses that are representative of very large areas and then reflect truth about our global atmosphere. For further information on the measures of CO<sub>2</sub> levels on *Mauna Loa*, the reader is referred to [14][15][16][17].

As shown in Fig. 1, the behavior of the GMSL variability is subject to significant rise during the altimetry era. The GMSL is also subject to significant seasonal variations. Global average surface temperatures clearly show that the Earth is subject of a global warming (see Fig. 2). The average temperature anomalies vary widely over decadal and interannual timescales.

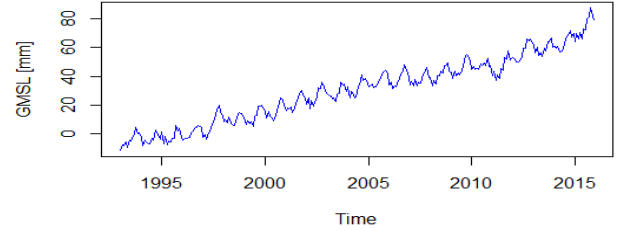


Figure 1. Global Mean Sea Level series.

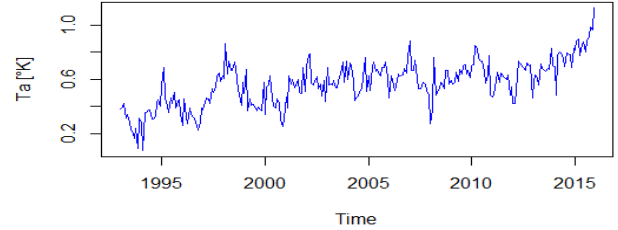


Figure 2. Global Mean Temperature Anomalies.

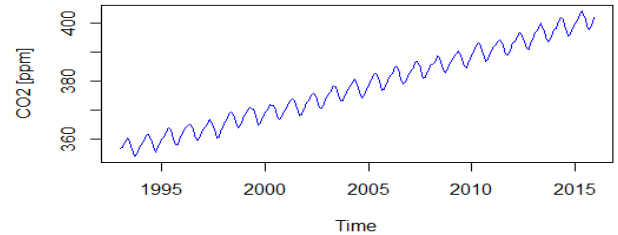


Figure 3. CO<sub>2</sub> concentrations measured at *Mauna Loa*.

As shown in Fig. 3, the levels of carbon dioxide in the atmosphere rise from October to May and fall each year every May to October as plants, through photosynthesis and respiration, take up the gas in spring and summer, and release it in fall and winter. The range of that cycle is expanding as more carbon dioxide is emitted from burning fossil fuels and other human activities.

### IV. RESULTS

In this Section, we consider a multivariate system composed by the three series: Global mean sea level, Global land-ocean mean temperature anomalies and CO<sub>2</sub> concentrations measured at *Mauna Loa*. These three time series, available under the KNMI Climate Explorer website (Royal Netherlands Meteorological Institute), cover a common period from January 1993 to the end of 2015, with a sampling rate of 1 month. This multivariate system, with a length of  $N = 276$ , is decomposed into trend, harmonic and residual components using the MSSA technique. The results of implementation of MSSA are obtained by means of the R package *Rssa* [18].

#### A. Decomposition and Information for Grouping

The window length  $L$  is the only parameter in the decomposition stage. Selection of the proper window length depends on the problem in hand and on preliminary information about the time series. Theoretical results tell us that  $L$  should be large enough but not greater than  $N/2$ .

Furthermore, if we know that the time series may have a periodic component with a given periodicity (for example a seasonal signal), then to get better separability of this periodic component it is advisable to take the window length proportional to that periodicity [19]. Following this approach and assuming that there is a dominant annual periodicity in the three series (see, Fig. 1, 2 and 3), the value of  $L$  is set at 132.

The third step of SSA or MSSA technique demands the grouping to make subgroups of the decomposed trajectory matrix and diagonal averaging to reconstruct the new time series from the subgroups. The separability, which characterizes how well different components can be separated from each other, is necessary to support this grouping step. A natural hint for grouping is the matrix of the absolute values of the w-correlations, corresponding to the full decomposition (in this decomposition each group corresponds to only one matrix component of the SVD) [20][21]. If the absolute value of the w-correlations is small, then the corresponding series are almost w-orthogonal, but, if it is large, then the two series are far from being w-orthogonal and are therefore badly separable [20][21].

The matrix of absolute values of w-correlations in Fig. 4 is depicted in gray scale from white to black corresponding to the absolute values of correlations from 0 to 1. As shown in Fig. 4, the block of 12–50 components is “gray” (large values of w-correlations); therefore, we can expect that these components are mixed and are produced by noise. Based on this information, we select the first 12 components for the identification of the harmonic and trend components and consider the rest as noise.

### B. Harmonic Components Identification

In practice, the singular values of the two eigentriples of a harmonic series are often very close to each other, and this fact simplifies the visual identification of the harmonic components. Therefore, explicit plateau in the eigenvalue spectra prompts the ordinal numbers of the paired eigentriples of harmonic components. Another way to identify the harmonic components of the series is to examine the pairwise scatterplots of the singular vectors. Pairwise scatterplots like spiral circles, spiral regular polygons or stars determine periodic components of the time series provided these components are separable from the residual component.

As shown in Fig. 5, there are two evident pairs with almost equal leading singular values, corresponding to two harmonic components: (3-4) and (10-11). For more evaluation, we also consider the 2D scatterplots of the first 12 paired eigenvectors. Fig. 6 shows that the pairs (3-4) and (10-11) are produced by modulated sine-waves, since the corresponding 2D-scatterplots of eigenvectors are similar to regular polygons. The periodicities of the two paired harmonic components (3-4 and 10-11) are: 12.004 months (annual signal) and 5.571 months (semi-annual signal), respectively.

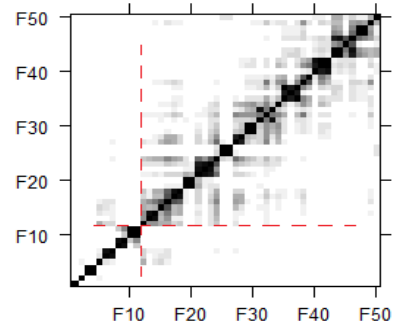


Figure 4. Matrix of weighted correlations.

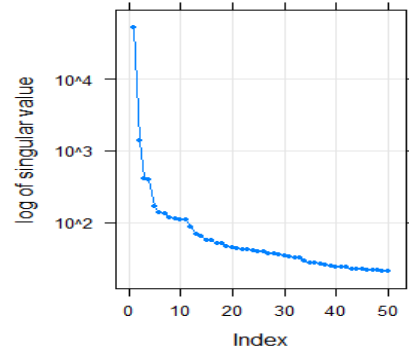


Figure 5. Logarithms of the first 50 eigenvalues.

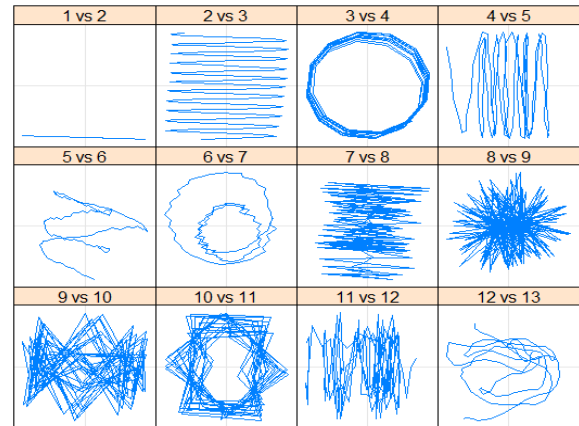


Figure 6. 2D scatterplots of the first 12 paired eigenvectors.

### C. Trend Identification

Within the framework of SSA, the trend is defined as a smooth component containing information about time series global change. Fig. 7 shows that the eigenvectors: 1, 2, 5, 6, 7 and 12, are slowly-varying and therefore, should be included in the trend group.

Fig. 8 represents the decomposition results obtained using the MSSA technique. The reconstructed trend indicates that the GMSL is subject to significant rise of 77.28 mm during the period 1993-2015. Applying a least squares linear regression analysis to the extracted trend gives a rate of 3.36 mm/year between 1993 and 2015.

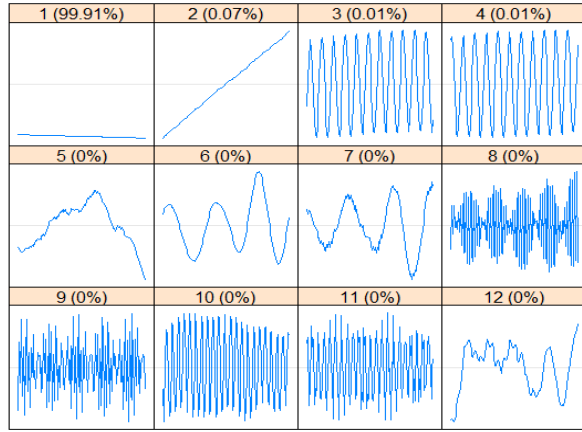


Figure 7. 1D graphs of the first 12 eigenvectors and its contribution.

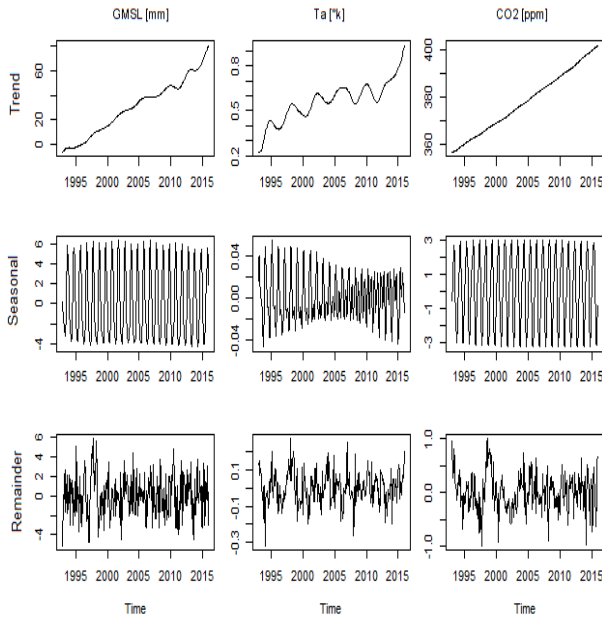


Figure 8. Trend, seasonality and Residuals: from left to right : Global mean sea level, temperature anomalies and CO<sub>2</sub> concentrations.

The GMSL trend shows that there are a number of fluctuations over short periods. This variability is at least partly related to El Nino/La Nina episodes (sea level rises during El Nino and falls during LaNina) and associated changes in the hydrological cycle [22]. The El Nino of 1997–98 was extremely severe. It started in April to May 1997, its effects extended into the early summer of 1998. The trend of global temperature dataset indicates the temperature of the globe combining land masses and oceans is subject to significant rise. A warming of 0.39 °K over the same period (1993-2015) is observed. The atmospheric CO<sub>2</sub> recordings at *Mauna Loa* show a clear increasing trend, due to the addition of anthropogenic gases. In March 2015, the mean concentration of CO<sub>2</sub> at *Mauna Loa* reached 400 ppm (trend data). Correlations between the three obtained trends confirm the relationship between observed interacting factors (see Table 1).

TABLE I. CORRELATION BETWEEN THE THREE TRENDS

Trend	Global Mean Sea Level	Temperature anomalies	CO <sub>2</sub> Concentrations
Global Mean Sea Level	-	0.91	0.99
Temperature anomalies	0.91	-	0.88
CO <sub>2</sub> Concentrations	0.99	0.88	-

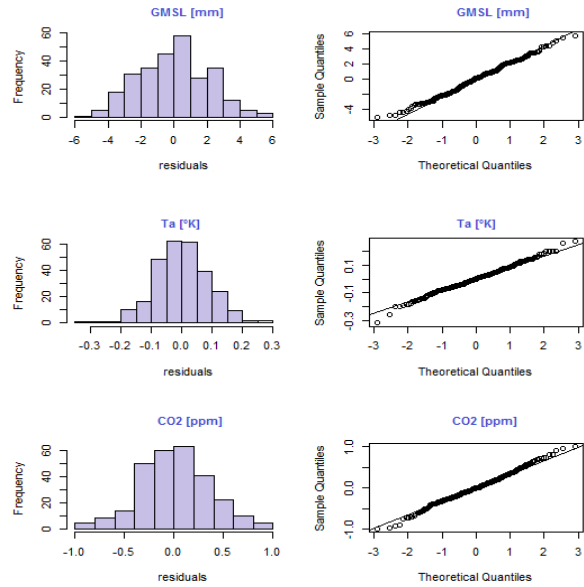


Figure 9. Histograms of residuals (left) and de Q-Q graphs (right): from top to bottom : Global mean sea level, temperature anomalies and CO<sub>2</sub> concentrations.

#### D. Residuals

Fig. 9 shows the histograms of residuals which are obtained from grouping of the eigentriples, which do not contain elements of trend and oscillations. The Q-Q graphs indicate that the normality of the residuals is not rejected.

#### V. CONCLUSION

The analysis by the method Multivariate Singular Spectrum Analysis (MSSA) of the multivariate system composed by three series: Global mean sea level , Global land-ocean mean temperature anomalies and CO<sub>2</sub> concentrations measured at *Mauna Loa*, has allowed us to connect and identify trends and seasonal patterns of these three indices. The obtained results may appear to be primary, but it is these "curves" of tendency which, for climatologists, are of paramount importance in the search for possible correlations between the climatic events that Earth undergoes.

During the period of last 23 years (1993-2015), data from satellite altimetry indicate that the global mean sea level has risen by 77.28 mm. The average rate of increase is of 3.36 mm/year between 1993 and 2015. Although the extracted global trend indicates a rise in the mean level of the oceans, there are marked fluctuations over short periods.

The globe combining land masses and oceans had, meanwhile, a warming of 0.39 °K over the same period. The average rate of increase in atmospheric CO<sub>2</sub> content recorded at *Mauna Loa* is 1.98 ppm/year over the period 1993-2015.

In conclusion, the MSSA is an excellent tool to decompose and reconstruct signal, such as the variations in the average level of the oceans and seas. The MSSA is an efficient analyzing means, especially when the multivariate series system represents connectable factors.

#### ACKNOWLEDGMENT

The author is very grateful to the Royal Netherlands Meteorological Institute for providing GMSL, NOAA's Merged Land-Ocean Surface Temperature and *Mauna Loa*'s CO<sub>2</sub> concentration time series. The author thanks also Dr. Nina Golyandina, Dr. Anton Korobeynikov, Dr. Alex Shlemov (St. Petersburg State University) and Konstantin Usevich (GIPSA-lab, CNRS) for providing the Rssa package. The author greatly appreciates the anonymous reviewers for their valuable and constructive comments.

#### REFERENCES

- [1] J. Fourier, "Résumé Théorique des Propriétés de la Chaleur Rayonnante," *Annales de Chimie et de Physique*, vol. 27, 1824, pp. 236-281.
- [2] S. Arrhenius, "On the Influence of Carbonic Acid in the Air upon the Temperature of the Ground," *Philosophical Magazine and Journal of Science*, vol. 5, no. 41, 1896, pp. 237-276. <http://www.globalwarmingart.com/images/1/18/Arrhenius.pdf>
- [3] R. Kahele, "Behind the Inconvenient Truth," *Hana Hou!*, vol. 10, no. 5, Octobre/Novembre 2007.
- [4] National Academy of Sciences, "Carbon Dioxide and Climate: A Scientific Assessment. Report of an Ad Hoc Study Group on Carbon Dioxide and Climate," Woods Hole, Massachusetts, July 23-27, to the Climate Research Board, Assembly of Mathematical and Physical Sciences, National Research Council, 1979. [Online] Available from: [http://people.atmos.ucla.edu/brianpm/download/charney\\_report.pdf](http://people.atmos.ucla.edu/brianpm/download/charney_report.pdf) [retrieved: March 2017].
- [5] IPCC - Intergovernmental Panel on Climate Change, "Assessment Reports," [Online] Available from: [http://www.ipcc.ch/publications\\_and\\_data/publications\\_and\\_data\\_reports.shtml](http://www.ipcc.ch/publications_and_data/publications_and_data_reports.shtml) [retrieved: March 2017].
- [6] EPICA Community Members, "Eight Glacial Cycles from an Antarctic Ice Core," *Nature*, vol. 429, 2004, pp. 623-628, doi:10.1038/nature02599
- [7] A. B. Robinson, N. Robinson, and A. Soon, "Environmental Effects of Increased Atmospheric Carbon Dioxide," *Journal of American Physicians and Surgeons*, vol. 12, 2007, pp. 79-90.
- [8] United Nations, "Kyoto Protocol to the United Nations Framework Convention on Climate Change," 1998, p.21. [Online] Available from: <https://unfccc.int/resource/docs/convkp/kpeng.pdf> [retrieved: March 2017].
- [9] N. Golyandina, V. Nekrutkin, and A. Zhigljavsky, "Analysis of Time Series Structure: SSA and Related Techniques," *Chapman & Hall/CRC*, doi:10.1201/9781420035841, 2001, p. 309.
- [10] N. Golyandina and D. Stepanov, "SSA-Based Approaches to Analysis and Forecast of Multidimensional Time Series," in *Proceedings of the 5th St. Petersburg Workshop on Simulation*, St. Petersburg State University, June 26-July 2, 2005, pp. 293-298.
- [11] R. S. Nerem, D. Chambers, C. Choe, and G. T. Mitchum, "Estimating Mean Sea Level Change from the TOPEX and Jason Altimeter Missions," *Marine Geodesy*, vol. 33, no. 1 supp 1, 2010, pp. 435-446, doi: 10.1080/01490419.2010.491031
- [12] T. M. Smith, R. W. Reynolds, T.C. Peterson, and J. Lawrimore, "Improvements to NOAA's Historical Merged Land-Ocean Surface Temperatures Analysis (1880-2006)," *Journal of Climate*, vol. 21, 2008, pp. 2283-2296, doi:10.1175/2007JCLI2100.1.
- [13] R. S. Vose, D. Arndt, V. F. Banzon, D. R. Easterling, B. Gleason, B. Huang, E. Kearns, J. H. Lawrimore, M. J. Menne, T. C. Peterson, R. W. Reynolds, T. M. Smith, C. N. Williams, Jr., and D.L. Wuertz, "NOAA's Merged Land-Ocean Surface Temperature Analysis," *Bulletin of the American Meteorological Society*, vol. 93, 2012, pp. 1677-1685, doi:10.1175/BAMS-D-11-00241.1.
- [14] W. D. Komhyr, T. B. Harris, L. S. Waterman, J. F. S. Chin, and K. W. Thoning, "Atmospheric Carbon Dioxide at Mauna Loa Observatory 1. NOAA Global Monitoring for Climatic Change Measurements with a nondispersive infrared analyzer, 1974-85," *Journal of Geophysical Research*, vol. 94, 1989, pp. 8533-8547, doi:10.1029/JD094iD06p08533.
- [15] K. W. Thoning, P. P. Tans, and W. D. Komhyr, "Atmospheric Carbon Dioxide at Mauna Loa Observatory 2. Analysis of the NOAA GMCC data, 1974-1985," *Journal of Geophysical Research*, vol. 94, 1989, pp. 8549-8565, doi:10.1029/JD094iD06p08549.
- [16] C. L. Zhao and P. P. Tans, "Estimating Uncertainty of the WMO Mole Fraction Scale for Carbon Dioxide in Air," *Journal of Geophysical Research*, vol. 111, D08207, doi: 10.1029/2005JD006003, 2006.
- [17] C. Zhao, P.P. Tans, and K.W. Thoning, "A High Precision Manometric System for Absolute Calibrations of CO<sub>2</sub> in dry air," *Journal of Geophysical Research*, vol. 102, 1997, pp. 5885-5894, doi:10.1029/96JD03764.
- [18] N. Golyandina, A. Korobeynikov, A. Shlemov, and K. Usevich, "Multivariate and 2D Extensions of Singular Spectrum Analysis with the Rssa Package," *Journal of Statistical Software*, vol. 67, no 2, 2015, p.78, doi: 10.18637/jss.v067.i02.
- [19] H. Hassani, R. Mahmoudvand, and M. Yarmohammadi, "Filtering and Denoising in the Linear Regression Model," *Fluctuation and Noise Letters*, vol. 9, no. 4, 2010, pp. 343-358, doi: 10.1142/S0219477510000289.
- [20] H. Hassani, "Singular Spectrum Analysis: Methodology and Comparison," *Journal of Data Science*, vol. 5, no 2, 2007, pp. 239-257.
- [21] H. Hassani, "A Brief Introduction to Singular Spectrum Analysis," unpublished. [Online] Available from: [http://www.ssa.cf.ac.uk/a\\_brief\\_introduction\\_to\\_ssa.pdf](http://www.ssa.cf.ac.uk/a_brief_introduction_to_ssa.pdf) [retrieved: March 2017].
- [22] M. Haddad, H. Taibi, and S. M. Mohammed Arezki, "On the Recent Global Mean Sea Level Changes: Trend extraction and El Nino's Impact," *Comptes Rendus Geoscience*, vol. 345, no 4, 2013, pp. 167-175, doi :10.1016/j.crte.2013.03.002.